

Janet M. S. Skakle,^a John N. Low,^a James L. Wardell^b and Christopher Glidewell^{c*}

^aDepartment of Chemistry, University of Aberdeen, Meston Walk, Old Aberdeen AB24 3UE, Scotland, ^bInstituto de Química, Departamento de Química Inorgânica, Universidade Federal do Rio de Janeiro, CP 68563, 21945-970 Rio de Janeiro-RJ, Brazil, and ^cSchool of Chemistry, University of St Andrews, St Andrews, Fife KY16 9ST, Scotland

‡ Postal address: School of Engineering & Physics, University of Dundee, Dundee DD1 4HN, Scotland.

Correspondence e-mail: cg@st-andrews.ac.uk

Concomitant polymorphism and a temperature-dependent phase change in (*E*)-[1-(4-methoxyphenyl)-3-phenyl-2-propenylideneamino]oxyacetic acid

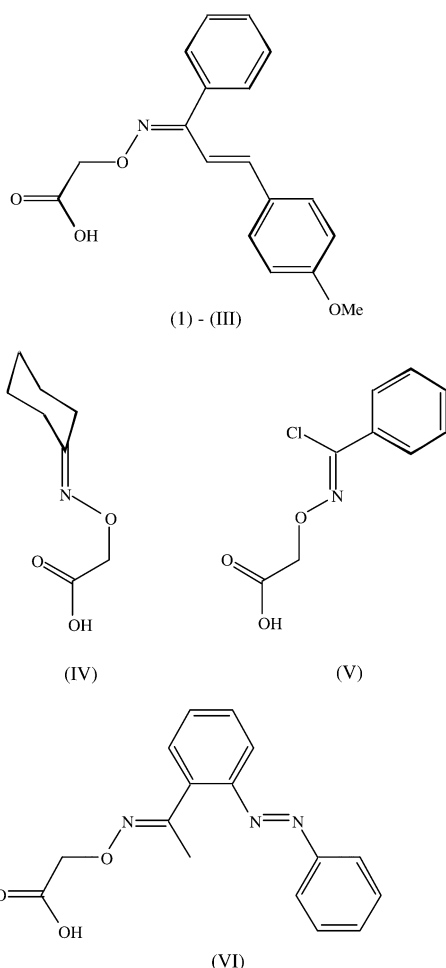
Received 25 October 2004

Accepted 23 February 2005

The title compound, C₁₈H₁₇NO₄, crystallizes from ethanol at ambient temperature as two concomitant polymorphs (I) and (II), both monoclinic *P*2₁/*c* with *Z*' = 1. The less abundant form (I) undergoes a reversible phase-transition at *ca* 173 K to a third monoclinic polymorph (III), *P*2₁/*n*, with *Z*' = 2, while the more abundant polymorph (II) is unchanged down to 120 K. In each polymorph of (I)–(III) the molecules are linked by pairs of O–H···O hydrogen bonds into cyclic dimers which are crystallographically centrosymmetric in (I) and (II), and approximately, but not crystallographically, centrosymmetric in (III). There are no direction-specific interactions between the hydrogen-bonded dimers in polymorph (I); in polymorph (II) the dimers are linked into sheets by C–H···N and C–H···π(arene) hydrogen bonds; in polymorph (III) the dimers are linked into chains by a C–H···π(arene) hydrogen bond. The interconversion of polymorphs (I) and (III) is a simple displacive phase transition.

1. Introduction

Persulfate oxidation of imino-oxyacetic acids, R¹R²C=NOCH₂COOH, provides a useful route to iminyl radicals (Forrester *et al.*, 1979). The subsequent reactions of the iminyl radicals thus generated depend greatly on the substituents and important species including nitrogen-containing heterocycles can result. We have recently reported the molecular and supramolecular structures of several substituted imino-oxyacetic acids, where the principal mode of supramolecular aggregation is the formation of the cyclic hydrogen-bonded dimers characteristic of simple carboxylic acids (Glidewell *et al.*, 2004*a,b*). Continuing this study, we have now investigated the title compound which proves to occur in several polymorphic forms. When the title compound was crystallized from ethanol, a mixture of two crystalline forms, concomitant polymorphs (Bernstein *et al.*, 1999), was obtained. These two forms, denoted (I) and (II), are both monoclinic at ambient temperature, with *Z*' = 1 in space group *P*2₁/*c*; while they have similar unit-cell volumes, their cell dimensions differ markedly and the polymorph with the longer *a* dimension we denote as polymorph (I). The structure of polymorph (II) has been determined both at 120 (2) and 291 (2) K, and these structure determinations, denoted (II*a*) and (II*b*), respectively, are essentially identical; hence, for this polymorph we only discuss the results of refinement (II*a*). However, when polymorph (I) is cooled to 120 (2) K, it forms a third monoclinic polymorph in *P*2₁/*n* with *Z*' = 2, denoted (III). The numbering of polymorphs (I)–(III) follows the order in which they were characterized. The supramolecular structures of polymorphs (I)–(III) are briefly compared with those of the analogous compounds (IV)–(VI).



2. Experimental

2.1. Synthesis

The title compound was prepared by the reaction of chloroacetic acid with the oxime derived from (*E*)-4-MeOC₆H₄CH=CHCOPh (Atmaram *et al.*, 1982); crystallization from ethanol at ambient temperature gave a mixture of polymorphs (I) and (II). Detailed X-ray examination of a representative sample of the crystals from this mixture indicated that the abundance ratio of (I):(II) was approximately 1:4.

2.2. Data collection, structure solution and refinement

Diffraction data for polymorph (I) and the data set for (II) denoted (I**b**) were collected on a Bruker SMART diffractometer at 291 (2) K; diffraction data for (III) and the dataset for (II) denoted (II**a**) were collected at 120 (2) K using a Nonius Kappa-CCD diffractometer: in all cases graphite-monochromated Mo *K*α radiation ($\lambda = 0.71073 \text{ \AA}$) was employed. Other details of cell data, data collection and refinement are summarized in Table 1, together with details of the software employed (Blessing, 1995, 1997; Bruker, 1998,

2000; Ferguson, 1999; McArdle, 2003; Nonius, 1997; Otwinowski & Minor, 1997; Sheldrick, 1997).

For polymorphs (I)–(III) the space groups $P2_1/c$, $P2_1/c$ and $P2_1/n$ were uniquely assigned from the systematic absences. The structures were solved by direct methods and refined with all data on F^2 . A weighting scheme based upon $P = [F_o^2 + 2F_c^2]/3$ was employed in order to reduce statistical bias (Wilson, 1976). All H atoms were located from difference maps and they were included in the refinements as riding atoms with distances C–H 0.93 Å (aromatic and ethylenic CH), 0.96 Å (CH₃) or 0.97 Å (CH₂) and O–H 0.82 Å at 291 (2) K, and C–H 0.95 Å (aromatic and ethylenic CH), 0.98 Å (CH₃) or 0.99 Å (CH₂) and O–H 0.84 Å at 120 (2) K, and with $U_{\text{iso}}(\text{H}) = 1.2U_{\text{eq}}(\text{C})$ or $1.5U_{\text{eq}}(\text{C},\text{O})$ for OH and methyl groups.

Supramolecular analyses were made and the diagrams were prepared with the aid of *PLATON* (Spek, 2003). Details of molecular conformations are given in Table 2 and details of hydrogen-bond dimensions are given in Table 3.¹ Figures 1–9 show the molecular components, with atom-labelling schemes, and aspects of the supramolecular structures.

2.3. Thermal analysis

DSC measurements were made using a Mettler Toledo model 821e instrument, with heating and cooling at a constant rate of 10 K per minute. The following thermal regime was adopted: samples were cooled from ambient temperature to 153 K and then held for 10 min, heated to 403 K and held for 10 min, cooled to 153 K and held for 10 min, heated to 423 K and held for 10 min, cooled to 153 K and held for 10 min, and finally heated to ambient temperature.

3. Results and discussion

3.1. Crystallization behaviour

An initial dataset collected at 291 (2) K gave a satisfactory solution and refinement for polymorph (I), but at this temperature only 27% of the reflections were labelled as ‘observed’: although these data were 99.1% complete to $\theta = 32.58\%$, with an overall data:parameter ratio of 28.4, the ratio of ‘observed’ data to parameters was only 7.5. Accordingly, a second dataset was collected at 120 (2) K using a freshly mounted crystal: this proved to have a different unit cell and a different supramolecular structure from that found from the first data set, and hence this form was denoted as polymorph (II). The observation of different structures derived from diffraction data collected from different crystals at different temperatures immediately raised the question of whether forms (I) and (II) were concomitant polymorphs both present in the original crystalline product, or whether a phase change from (I) to (II) had occurred upon cooling from 291 to 120 K.

Some ten crystals from the original batch were then taken, essentially at random, and their unit-cell dimensions were

¹ Supplementary data for this paper are available from the IUCr electronic archives (Reference: WS5022). Services for accessing these data are described at the back of the journal.

Table 1
Experimental details.

	(I)	(IIa)	(IIb)	(III)
Crystal data				
Chemical formula	C ₁₈ H ₁₇ NO ₄	C ₁₈ H ₁₇ NO ₄	C ₁₈ H ₁₇ NO ₄	C ₁₈ H ₁₇ NO ₄
<i>M_r</i>	311.33	311.33	311.33	311.33
Cell setting, space group	Monoclinic, <i>P2₁/c</i>	Monoclinic, <i>P2₁/c</i>	Monoclinic, <i>P2₁/c</i>	Monoclinic, <i>P2₁/n</i>
<i>a</i> , <i>b</i> , <i>c</i> (Å)	8.5153 (7), 16.0591 (13), 12.1476 (10)	6.4499 (2), 14.9693 (5), 16.6559 (6)	6.4238 (3), 15.1513 (9), 17.0552 (9)	12.1552 (4), 15.8657 (4), 16.6708 (5)
β (°)	96.801 (2)	92.947 (2)	93.167 (2)	97.4250 (15)
<i>V</i> (Å ³)	1649.5 (2)	1606.01 (9)	1657.43 (15)	3188.02 (16)
<i>Z</i> , <i>Z'</i>	4, 1	4, 1	4, 1	8, 2
<i>D_x</i> (Mg m ⁻³)	1.254	1.288	1.248	1.297
Radiation type	Mo <i>K</i> α	Mo <i>K</i> α	Mo <i>K</i> α	Mo <i>K</i> α
No. of reflections for cell parameters	5963	3690	3837	7291
θ range (°)	2.1–32.6	3.0–27.5	1.8–27.6	3.1–27.5
μ (mm ⁻¹)	0.09	0.09	0.09	0.09
Temperature (K)	291 (2)	120 (2)	291 (2)	120 (2)
Crystal form, colour	Plate, colourless	Plate, yellow	Plate, colourless	Lath, colourless
Crystal size (mm)	0.45 × 0.40 × 0.04	0.25 × 0.20 × 0.05	0.25 × 0.20 × 0.05	0.50 × 0.40 × 0.10
Data collection				
Diffractionmeter	Bruker SMART 1000 CCD area detector	Kappa-CCD	Bruker SMART 1000 CCD area detector	Bruker–Nonius 95 mm CCD camera on κ -goniostat
Data collection method	φ - ω	φ scans, and ω scans with κ offsets	φ - ω	φ and ω scans
Absorption correction				
<i>T_{min}</i>	0.952	0.967	0.982	0.950
<i>T_{max}</i>	0.996	0.995	0.996	0.991
No. of measured, independent and observed reflections	16 995, 5963, 1586	17 758, 3690, 2647	13 953, 3837, 2171	37 246, 7291, 4714
Criterion for observed reflections	<i>I</i> > 2 σ (<i>I</i>)	<i>I</i> > 2 σ (<i>I</i>)	<i>I</i> > 2 σ (<i>I</i>)	<i>I</i> > 2 σ (<i>I</i>)
<i>R_{int}</i>	0.058	0.062	0.038	0.060
θ_{\max} (°)	32.6	27.5	27.6	27.5
Range of <i>h</i> , <i>k</i> , <i>l</i>	-12 \Rightarrow <i>h</i> \Rightarrow 12 -16 \Rightarrow <i>k</i> \Rightarrow 24 -17 \Rightarrow <i>l</i> \Rightarrow 18	-8 \Rightarrow <i>h</i> \Rightarrow 8 -19 \Rightarrow <i>k</i> \Rightarrow 19 -21 \Rightarrow <i>l</i> \Rightarrow 16	-7 \Rightarrow <i>h</i> \Rightarrow 8 -19 \Rightarrow <i>k</i> \Rightarrow 19 -22 \Rightarrow <i>l</i> \Rightarrow 21	-15 \Rightarrow <i>h</i> \Rightarrow 15 -20 \Rightarrow <i>k</i> \Rightarrow 20 -21 \Rightarrow <i>l</i> \Rightarrow 21
Refinement				
Refinement on	<i>F</i> ²	<i>F</i> ²	<i>F</i> ²	<i>F</i> ²
<i>R</i> [<i>F</i> ² > 2 σ (<i>F</i> ²)], <i>wR</i> (<i>F</i> ²), <i>S</i>	0.056, 0.172, 0.86	0.058, 0.232, 1.14	0.049, 0.151, 0.98	0.048, 0.133, 1.03
No. of reflections	5963	3690	3837	7291
No. of parameters	210	210	210	419
H-atom treatment	Constrained to parent site	Constrained to parent site	Constrained to parent site	Constrained to parent site
Weighting scheme	$w = 1/[\sigma^2(F_o^2) + (0.0654P)^2]$, where $P = (F_o^2 + 2F_c^2)/3$	$w = 1/[\sigma^2(F_o^2) + (0.1318P)^2 + 0.4171P]$, where $P = (F_o^2 + 2F_c^2)/3$	$w = 1/[\sigma^2(F_o^2) + (0.0795P)^2 + 0.0527P]$, where $P = (F_o^2 + 2F_c^2)/3$	$w = 1/[\sigma^2(F_o^2) + (0.0728P)^2 + 0.0298P]$, where $P = (F_o^2 + 2F_c^2)/3$
(Δ/σ) _{max}	<0.0001	<0.0001	<0.0001	0.001
$\Delta\rho_{\max}$, $\Delta\rho_{\min}$ (e Å ⁻³)	0.14, -0.12	0.66, -0.64	0.15, -0.14	0.19, -0.27

Computer programs used: SMART (Bruker, 1998), Kappa-CCD server software (Nonius, 1997), COLLECT (Hooft, 1999), SAINT (Bruker, 2000), DENZO-SMN (Otwinowski & Minor, 1997), DENZO (Otwinowski & Minor, 1997), SHELXS97 (Sheldrick, 1997), OSCAIL (McArdle, 2003), PRPKAPPA (Ferguson, 1999).

determined at 291 K: the majority were of polymorph (II) but several of the crystals were of polymorph (I), confirming the occurrence of concomitant polymorphism at ambient temperature. Two further datasets were then collected, one for polymorph (II) at ambient temperature and a second at 120 (2) K for a crystal which had been shown to be of polymorph (I) at ambient temperature: this crystal at 120 K proved to have yet a third unit cell, having undergone a phase transformation upon cooling, and this form is denoted as polymorph (III).

DSC examination of the original mixture of polymorphs showed several distinct events as the temperature was cycled in the range 153–423 K (–120 to +150°C): a reversible phase

transition, corresponding to the interconversion of polymorphs (I) and (III), was observed at approximately 173 K, and the melting points of (I) and (II) were observed at 393 and 413 K, respectively. However, while the melting of (I) was reversible, cooling the melt of (II) led to the formation of a glass rather than to crystallization.

3.2. Molecular conformations

In each of the independent molecules in polymorphs (I)–(III) (Figs. 1–3) the intramolecular bond lengths and angles are very similar, and all distances have values which are typical of their types (Allen *et al.*, 1987). However, there are some

Table 2
Selected geometrical parameters (Å, °).

	(I)	(IIa)	(IIb)	(III) Mol. 1	(III) Mol. 2
Temperature (K)	291	120	291	120	120
<i>x</i>	Nil	Nil	Nil	1	2
Parameter					
Ox3–Nx4	1.417 (2)	1.421 (2)	1.4165 (18)	1.4214 (16)	1.4243 (16)
Nx4–Cx5	1.294 (2)	1.297 (3)	1.291 (2)	1.289 (2)	1.298 (2)
Cx2–Ox3–Nx4	107.08 (17)	108.30 (16)	108.14 (13)	107.10 (12)	107.72 (11)
Ox3–Nx4–Cx5	111.16 (17)	111.37 (17)	111.05 (14)	110.93 (13)	111.00 (12)
Ox1–Cx1–Cx2–Ox3	–177.8 (2)	–168.8 (2)	–168.96 (16)	–173.35 (14)	176.70 (13)
Cx1–Cx2–Ox3–Nx4	–153.1 (2)	–78.8 (2)	–80.63 (18)	–158.92 (13)	145.91 (13)
Cx2–Ox3–Nx4–Cx5	179.5 (2)	173.2 (2)	174.60 (15)	–177.91 (14)	–172.06 (13)
Ox3–Nx4–Cx5–Cx6	1.5 (3)	–1.1 (3)	–1.6 (2)	1.1 (2)	–0.3 (2)
Nx4–Cx5–Cx6–Cx7	171.7 (2)	168.7 (2)	169.29 (17)	172.97 (16)	–170.89 (15)
Nx4–Cx5–Cx11–Cx12	113.3 (2)	124.3 (2)	121.89 (19)	107.38 (19)	–119.08 (16)
Cx6–Cx7–Cx21–Cx22	10.5 (2)	2.4 (4)	2.8 (3)	8.3 (3)	–11.1 (3)
Cx23–Cx24–Ox24–Cx27	175.4 (2)	–179.1 (2)	–178.57 (18)	178.30 (14)	–173.96 (13)

significant variations in the molecular conformations, as shown by the key torsional angles (Table 2), although the torsional angles in polymorph (II) all show very little variation with temperature. For polymorph (III) the values of those torsional angles which are remote from zero or 180° generally have similar magnitudes for the two independent molecules but with opposite signs, indicating that the two molecules are close to being enantiomorphs and pointing up the pseudosymmetric nature of the hydrogen-bonded dimer (Fig. 3). The most notable variation between the different polymorphs occurs in the torsional angle Cx1–Cx2–Ox3–Nx4, where polymorph (II) adopts quite a different value from those in polymorphs (I) and (III), where the values are, in fact, rather similar in magnitude.

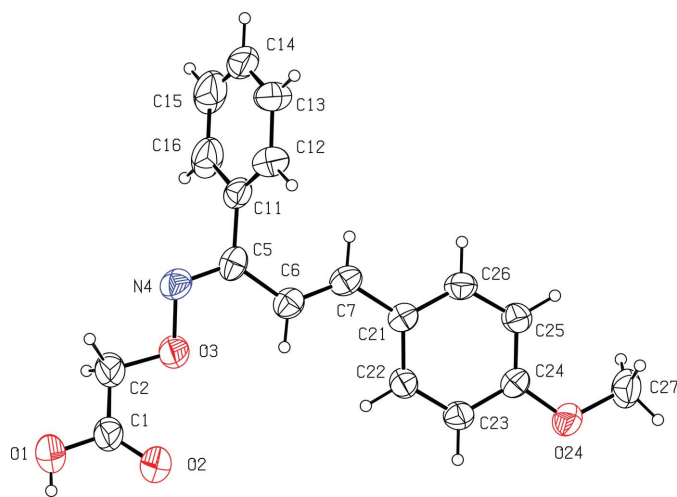


Figure 1
The molecule in polymorph (I) at 291 K showing the atom-labelling scheme. Displacement ellipsoids are drawn at the 30% probability level.

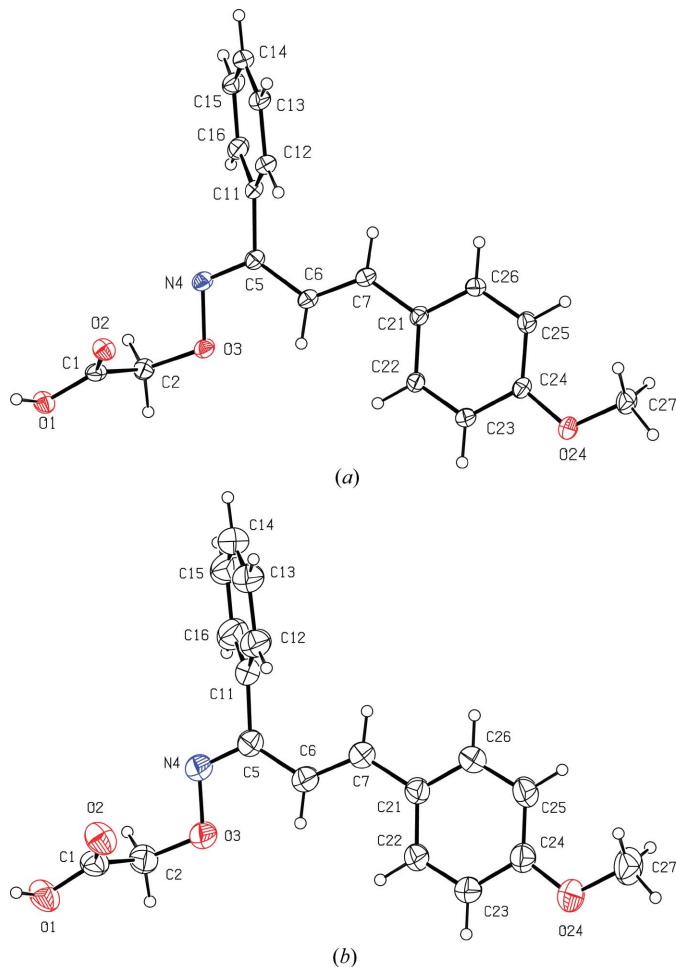


Figure 2
The molecule in polymorph (II) showing the atom-labelling scheme: (a) at 120 K (IIa) and (b) at 291 K (IIb). Displacement ellipsoids are drawn at the 30% probability level.

3.3. Supramolecular aggregation

In each polymorph the primary mode of supramolecular aggregation is the formation of $R_2^2(8)$ (Bernstein *et al.*, 1995) dimers by means of paired O–H...O hydrogen bonds (Table B): these dimers are centrosymmetric in polymorphs (I) and (II) (Figs. 4 and 5) and pseudosymmetric in polymorph (III), where the dimer contains one of each type of independent molecule (Fig. 3). In both (I) and (II) the reference molecule has been selected such that the hydrogen-bonded dimer is centred at $(\frac{1}{2}, \frac{1}{2}, \frac{1}{2})$; in (III) the selected asymmetric unit is approximately centrosymmetric and its centroid lies at approximately $(\frac{1}{2}, \frac{1}{2}, 0.22)$.

In polymorph (II) the dimers are linked into sheets by means of C–

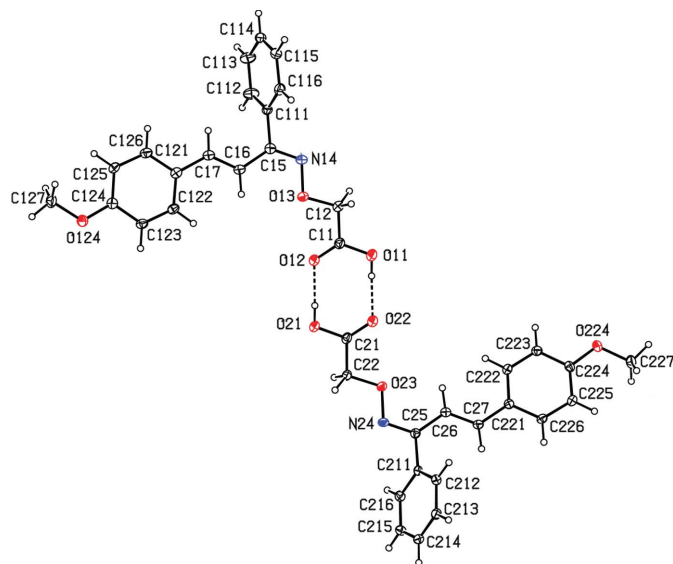
Table 3

Selected hydrogen bond parameters (Å, °).

$D-H \cdots A$	$H \cdots A$	$D \cdots A$	$D-H \cdots A$
(I)			
$O1-H1 \cdots O2^i$	1.85	2.662 (3)	171
(IIa)			
$O1-H1 \cdots O2^i$	1.83	2.668 (3)	173
$C23-H23 \cdots N4^{ii}$	2.48	3.409 (3)	166
$C22-H22 \cdots Cg1^{iii\dagger}$	2.85	3.647 (3)	142
(IIb)			
$O1-H1 \cdots O2^i$	1.86	2.679 (3)	175
$C23-H23 \cdots N4^{ii}$	2.56	3.472 (2)	167
$C22-H22 \cdots Cg1^{iii\dagger}$	2.94	3.712 (2)	141
(III)			
$O11-H11 \cdots O22$	1.81	2.6542 (17)	177
$O21-H21 \cdots O12$	1.80	2.6410 (17)	178
$C215-H215 \cdots Cg2^{iii‡}$	2.64	3.532 (2)	157

Symmetry codes: (i) $1-x, 1-y, 1-z$; (ii) $-x, \frac{1}{2}+y, \frac{1}{2}-z$; (iii) $\frac{3}{2}-x, -\frac{1}{2}+y, -\frac{1}{2}-z$. † Cg1 is the centroid of the C31–C36 ring. ‡ Cg2 is the centroid of the C221–C226 ring.

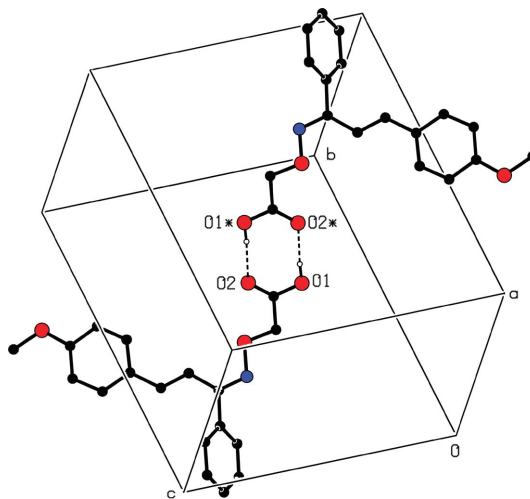
$H \cdots N$ hydrogen bonds, augmented by $C-H \cdots \pi$ (arene) hydrogen bonds, and the patterns of the hydrogen bonds are same at both 120 and 291 K, while the dimensions change only slightly between these two temperatures (Table 3). The atoms of type C23 in the molecules at (x, y, z) and $(1-x, 1-y, 1-z)$ are components of the $R_2^2(8)$ dimer centred at $(\frac{1}{2}, \frac{1}{2}, \frac{1}{2})$. These two atoms act as hydrogen-bond donors to the N4 atoms in the molecules at $(-x, \frac{1}{2}+y, \frac{1}{2}-z)$ and $(1+x, \frac{1}{2}-y, \frac{1}{2}+z)$, which lie respectively in the dimers centred at $(-\frac{1}{2}, 1, 0)$ and $(\frac{3}{2}, 0, 1)$. At the same time the atoms N4 at (x, y, z) and $(1-x, 1-y, 1-z)$ accept hydrogen bonds from the atoms C23 at $(-x, -\frac{1}{2}+y, \frac{1}{2}-z)$ and


Figure 3

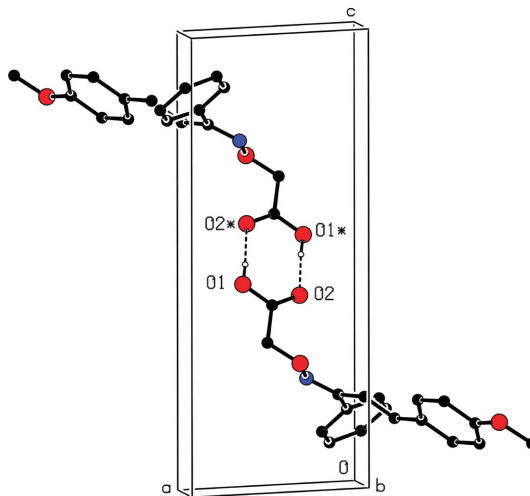
The two independent molecules in polymorph (III) at 120 K showing the atom-labelling scheme and the dimeric aggregate formed by the $O-H \cdots O$ hydrogen bonds. Displacement ellipsoids are drawn at the 30% probability level.

$(1+x, \frac{3}{2}-y, \frac{1}{2}+z)$, which themselves lie in the dimers centred at $(-\frac{1}{2}, 0, 0)$ and $(\frac{3}{2}, 1, 1)$, respectively. In this manner a $(10\bar{2})$ sheet is generated (Fig. 6), in which $O-H \cdots O$ and $C-H \cdots N$ hydrogen bonds generate $R_2^2(8)$ and $R_6^0(52)$ rings, which alternate in chessboard fashion. The $C-H \cdots \pi$ (arene) hydrogen bonds (Table 3) follow exactly the same pattern (Fig. 7) and hence serve to reinforce the sheet generated by the $C-H \cdots N$ hydrogen bonds.

By contrast, in polymorph (I) there are no hydrogen bonds between adjacent dimers: in particular, the $C-H \cdots N$ and $C-H \cdots \pi$ (arene) hydrogen bonds found in polymorph (II) are both absent from the crystal structure of (I). The only direction-specific interaction of possible significance between the


Figure 4

Part of the crystal structure of polymorph (I) at 291 K showing the formation of a centrosymmetric $R_2^2(8)$ dimer. For the sake of clarity, the H atoms bonded to C atoms have been omitted. The atoms marked with an asterisk (*) are at the symmetry position $(1-x, 1-y, 1-z)$.


Figure 5

Part of the crystal structure of polymorph (II) at 120 K showing the formation of a centrosymmetric $R_2^2(8)$ dimer. For the sake of clarity, the H atoms bonded to C atoms have been omitted. The atoms marked with an asterisk (*) are at the symmetry position $(1-x, 1-y, 1-z)$.

$R_2^2(8)$ dimers in (I) is a weak $\pi \cdots \pi$ stacking interaction. The methoxy-substituted rings C21–C26 in the molecules at (x, y, z) and $(-x, 1 - y, 2 - z)$ are strictly parallel, but both the interplanar spacing, 3.534 (2) Å, and the ring-centroid separation, 3.960 (2) Å, are rather large, associated with a large centroid offset of 1.787 (2) Å; hence, this interaction is probably not structurally significant.

The principal interaction between the dimeric units in polymorph (III) is a C–H $\cdots\pi$ (arene) hydrogen bond which involves only the molecules of type 2 (containing C21 *etc.*). The aryl C215 atom in the unsubstituted ring of the type 2 molecule at (x, y, z) acts as a hydrogen-bond donor to the substituted ring C221–C216 in the corresponding molecule at $(\frac{3}{2} - x, -\frac{1}{2} + y, -\frac{1}{2} - z)$, so forming a chain of type 2 molecules, from which the type 1 molecules are pendent, running parallel to the [010] direction and generated by the 2_1 screw axis along $(\frac{3}{4}, y, -\frac{1}{4})$, see Fig. 8. As in polymorph (I), the $\pi \cdots \pi$ stacking interactions in (III) again involve the methoxy-substituted rings, in particular those of type 2 molecules at (x, y, z) and $(2 - x, 1 - y, -z)$, see §3.4. Also as in (I), the large interplanar separations and large ring-centroid separations (> 3.8 Å) indicate that these interactions are probably not structurally significant.

3.4. Phase relationship

The relationship between the crystal structures of polymorphs (I) and (III) can readily be understood once it is recognized that the unit cell of (III) can be derived from that of (II) *via* the transformation $(0, 0, 1; 0, -1, 0; 2, 0, 0)$. In polymorph (I) the dimeric units are centred at $(\frac{1}{2}, \frac{1}{2}, \frac{1}{2})$ and $(\frac{1}{2}, 0, 0)$, whereas in (III), where the length of the c axis is double that of the a axis in (I), the dimers are located at approximately $(\frac{1}{2}, \frac{1}{2}, 0.22)$, $(\frac{1}{2}, \frac{1}{2}, 0.78)$, $(0, 0, 0.28)$ and $(0, 0, 0.72)$, leading to a very close similarity between the structures of (I) and (III) (Fig. 9). Hence, this temperature-dependent change of structure from $P2_1/c$ with $Z' = 1$ at 291 K, to $P2_1/n$ with $Z' = 2$ at 120 K can be described as a simple displacive transition. The similarity of molecular conformation between the unique molecules in polymorph (I), and each of the two independent

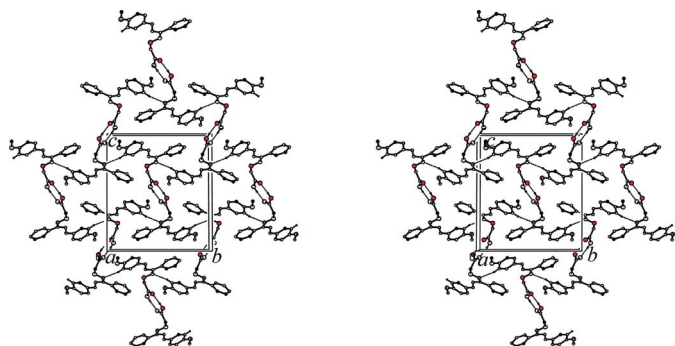


Figure 6
Stereoview of part of the crystal structure of polymorph (II) at 120 K showing the formation of a $(10\bar{2})$ hydrogen-bonded sheet of $R_2^2(8)$ and $R_6^0(52)$ rings built from O–H \cdots O and C–H \cdots N hydrogen bonds. For the sake of clarity the H atoms not involved in the motifs shown have been omitted.

molecules in (III), is entirely consistent with this. In both (I) and (III) the pattern of the hard (Braga *et al.*, 1995) hydrogen bonds is essentially the same and the difference between the supramolecular structures of (I) and (III) depends on a single rather weak C–H $\cdots\pi$ (arene) hydrogen bond in (III), which is absent from the structure of (I).

3.5. Comparison with analogous structures

It is of interest to compare briefly the supramolecular structures of polymorphs (I)–(III) with those of the related compounds (IV)–(VI) (Glidewell *et al.*, 2004*a,b*). In each of (IV)–(VI), the molecules are linked by paired O–H \cdots O hydrogen bonds into centrosymmetric dimers, analogous to those observed in (I) and (II), and in both (IV) and (VI) there are no direction-specific interactions between these dimers: in (V), on the other hand, the dimers are weakly linked into chains by a single aromatic $\pi \cdots \pi$ stacking interaction. It is noteworthy that C–H \cdots N hydrogen bonds are absent from the structures of each of (IV)–(VI), in contrast to polymorph (II).

3.6. General comments

In our recent structural studies we have encountered several examples of concomitant polymorphism. Thus, when crystallized from ethanol, 2-iodo-4-nitro aniline yields a mixture of triclinic ($P\bar{1}$, $Z' = 1$) and orthorhombic ($Pbca$, $Z' =$

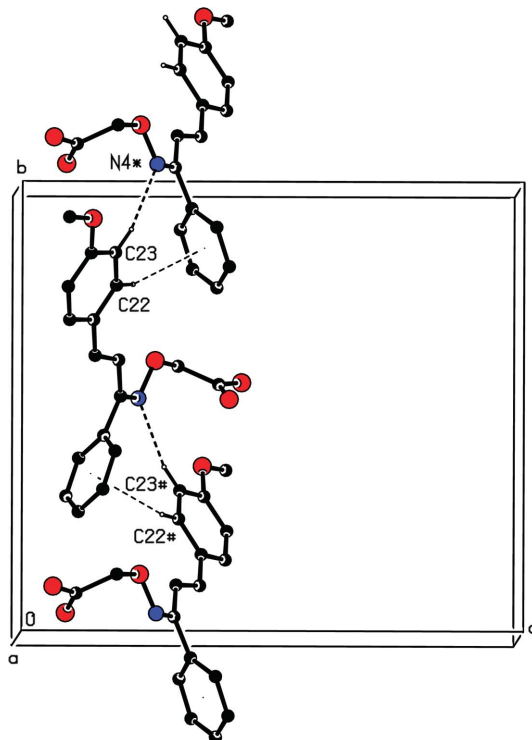


Figure 7
Part of the crystal structure of polymorph (II) at 120 K showing the cooperative combination of the C–H \cdots N and C–H $\cdots\pi$ (arene) hydrogen bonds. For the sake of clarity the H atoms not involved in the motifs shown have been omitted. The atoms marked with an asterisk (*) or a hash (#) are at the symmetry positions $(-x, \frac{1}{2} + y, \frac{1}{2} - z)$ and $(-x, -\frac{1}{2} + y, \frac{1}{2} - z)$, respectively.

1) crystals which have slightly different colours (McWilliam *et al.*, 2001); crystallization of ethyl *N*-(2-amino-6-benzyloxy-5-nitrosopyrimidin-2-yl)-3-aminopropanoate from acetonitrile/ethanol/water (1/1/1 by volume) yields a mixture of two monoclinic polymorphs, one blue ($P2_1/c$, $Z' = 1$) and the other pink ($P2_1$, $Z' = 2$; Quesada *et al.*, 2002), where the conformations of the three independent molecules of the nitrosopyrimidine are all different, so that these concomitant polymorphs are also conformational polymorphs; the 1:1 adduct formed between (*S*)-malic acid and 4,4'-bipyridyl crystallizes from methanol as a mixture of triclinic ($P\bar{1}$, $Z' = 1$) and monoclinic ($C2$, $Z' = 1$) polymorphs (Farrell *et al.*, 2002); benzanilide crystallizes from ethanol in both a monoclinic ($C2/c$, $Z' = 0.5$) form (Kashino *et al.*, 1979) and a triclinic ($P\bar{1}$, $Z' = 1$) form (Bowes, Glidewell *et al.*, 2003); the 2:1 adduct formed between triphenylsilanol and 4,4'-bipyridyl forms three triclinic polymorphs (all $P\bar{1}$ with $Z' = 0.5, 1$ and 4), which crystallize in pairwise-concomitant fashion (Bowes, Ferguson *et al.*, 2003); and crystallization of 1-(6-amino-1,3-benzodioxol-5-yl)-3-(4-methoxyphenyl)prop-2-en-1-one from dimethylformamide solution gives a mixture of a red monoclinic ($P2_1/c$, $Z' = 1$) polymorph and a yellow triclinic ($P\bar{1}$, $Z' = 2$) form, where the two independent molecules in the triclinic form exhibit different conformations, so providing a second example of conformational polymorphism also (Low *et al.*, 2004).

We emphasize that in none of these systems had there been any attempt to engineer such polymorphic behaviour, nor was this behaviour being specifically sought after: instead, each pair of polymorphs was identified serendipitously. In the cases of 2-iodo-4-nitroaniline, the nitrosopyrimidine and the substituted propenone, the identification of the two forms was facilitated by their differences in colour, but in the other examples identification depended solely upon careful scrutiny of the crystalline samples and observation of more than one crystal habit, followed in every case by careful manual separation. Our identification, essentially by chance, of seven

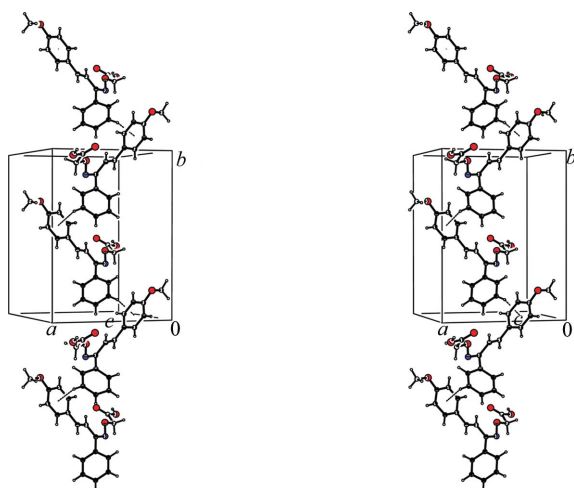


Figure 8
Stereoview of part of the crystal structure of polymorph (III) showing the formation of an [010] chain built of type 2 molecules only.

such examples within a rather short space of time suggests to us that the phenomenon of concomitant polymorphism may, in fact, be a rather common one, certainly far more common than the current literature (Bernstein *et al.*, 1999) tends to suggest, but one which goes largely un-noticed. On the other hand, we note the recent reports on 3,6,13,16-tetrabromo-2,7,12,17-

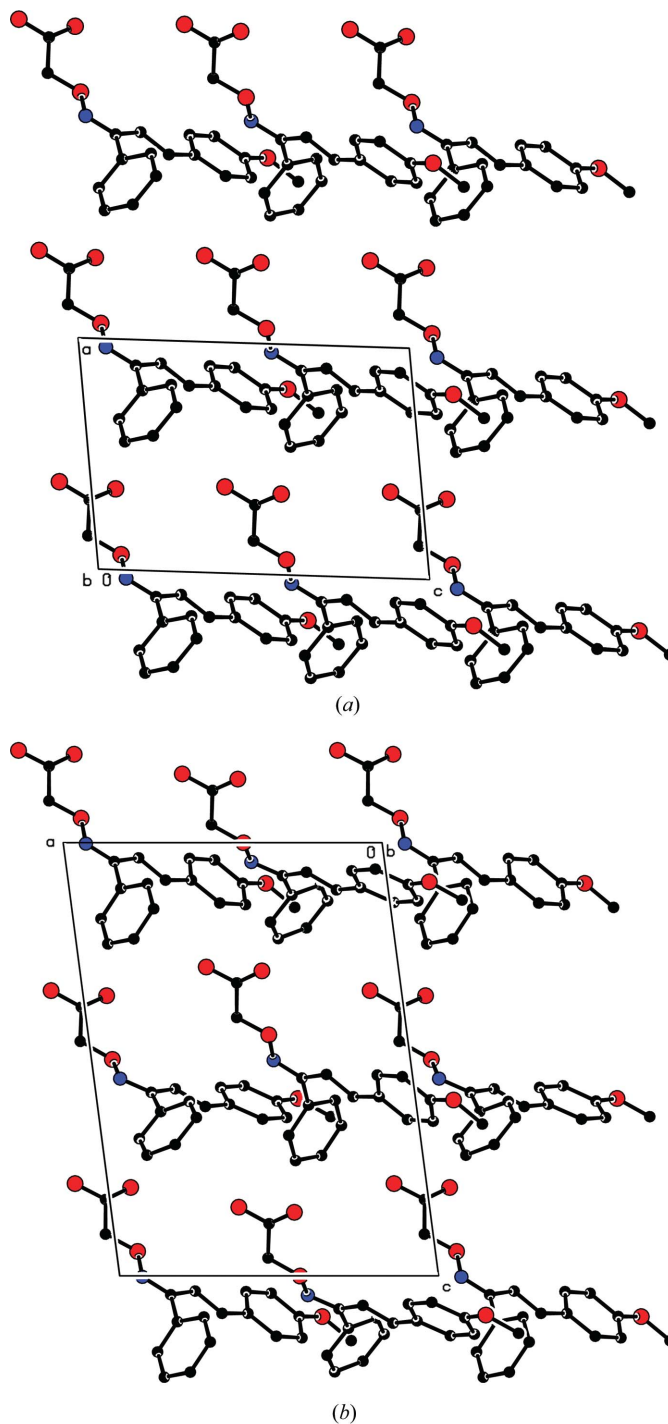


Figure 9
(a) Projection of part of the crystal structure of polymorph (I) in the domain $0 < y < \frac{1}{2}$; (b) projection of part of the crystal structure of polymorph (III) in the domain $\frac{1}{2} < y < 1.0$. For the sake of clarity, the other half of the unit-cell contents has been omitted in each case, as have the H atoms.

tetrapropylporphycene, where monoclinic prisms and triclinic plates crystallize concurrently from dichloromethane–hexane (Aritome *et al.*, 2002), and on the 1:1 co-crystal of caffeine and glutaric acid, where monoclinic rods and triclinic blocks crystallize concurrently from chloroform solution (Trask *et al.*, 2004).

4. Concluding remarks

The investigation of the title compound was originally expected to be entirely straightforward, simply providing another example of this class of compound for comparison with the analogues which have been reported recently (Glidewell *et al.*, 2004*a,b*). In the event, this investigation has proved to be much more complex than those for the previous examples. We emphasize, however, that as with so many examples of polymorphism, and particularly concomitant polymorphism, the structural behaviour can be unravelled, as here, only by careful and painstaking separation of a substantial number of individual crystals followed by their X-ray examination initially at ambient temperature and then at reduced temperature.

X-ray data for (IIa) and (III) were collected at the EPSRC X-ray Crystallographic Service, University of Southampton, UK. The authors thank the staff of the service for all their help and advice. X-ray data for (I) and (IIb) were collected at the University of Aberdeen using a Bruker SMART 1000CCD diffractometer and the authors thank the University of Aberdeen for funding the purchase of the diffractometer. JNL thanks NCR Self-Service, Dundee, for grants which have provided computing facilities for this work. JLW thanks CNPq and FAPERJ for financial support.

References

- Allen, F. H., Kennard, O., Watson, D. G., Brammer, L., Orpen, A. G. & Taylor, R. (1987). *J. Chem. Soc. Perkin Trans. 2*, pp. S1–S19.
- Aritome, I., Shimakoshi, H. & Hisaeda, Y. (2002). *Acta Cryst. C* **58**, o563–o564.
- Atmaram, S., Forrester, A. R., Gill, M., Napier, R. J. & Thomson, R. H. (1982). *Acta Chem. Scand. B*, **36**, 641–647.
- Bernstein, J., Davey, R. J. & Henck, J.-O. (1999). *Angew. Chem. Int. Ed.* **38**, 3440–3461.
- Bernstein, J., Davis, R. E., Shimoni, L. & Chang, N.-L. (1995). *Angew. Chem. Int. Ed. Engl.* **34**, 1555–1573.
- Blessing, R. H. (1995). *Acta Cryst. A* **51**, 33–37.
- Blessing, R. H. (1997). *J. Appl. Cryst.* **30**, 421–426.
- Bowes, K. F., Ferguson, G., Lough, A. J. & Glidewell, C. (2003). *Acta Cryst. B* **59**, 277–286.
- Bowes, K. F., Glidewell, C., Low, J. N., Skakle, J. M. S. & Wardell, J. L. (2003). *Acta Cryst. C* **59**, o1–o3.
- Braga, D., Grepioni, F., Birdha, K., Pedireddi, V. R. & Desiraju, G. R. (1995). *J. Am. Chem. Soc.* **117**, 3156–3166.
- Bruker (1998). *SMART*, Version 5.0. Bruker AXS Inc., Madison, Wisconsin, USA.
- Bruker (2000). *SADABS*, Version 2.03, and *SAINT*, Version 6.02a. Bruker AXS Inc., Madison, Wisconsin, USA.
- Farrell, D. M. M., Ferguson, G., Lough, A. J. & Glidewell, C. (2002). *Acta Cryst. B* **58**, 530–544.
- Ferguson, G. (1999). *PRPKAPPA*. University of Guelph, Canada.
- Forrester, A. R., Gill, M., Meyer, C. J., Sadd, J. S. & Thomson, R. H. (1979). *J. Chem. Soc. Perkin Trans. 1*, pp. 606–611.
- Glidewell, C., Low, J. N., Skakle, J. M. S. & Wardell, J. L. (2004*a*). *Acta Cryst. C* **60**, o270–o272.
- Glidewell, C., Low, J. N., Skakle, J. M. S. & Wardell, J. L. (2004*b*). *Acta Cryst. E* **60**, o1560–o1562.
- Hooft, R. W. W. (1999). *COLLECT*. Nonius BV, Delft, The Netherlands.
- Kashino, S., Ito, K. & Haisa, M. (1979). *Bull. Chem. Soc. Jpn.* **52**, 365–369.
- Low, J. N., Cobo, J., Noguera, M., Cuervo, P., Abonia, R. & Glidewell, C. (2004). *Acta Cryst. C* **60**, o744–o750.
- McArdle, P. (2003). *OSCAIL for Windows*, Version 10. Crystallography Centre, Chemistry Department, NUI Galway, Ireland.
- McWilliam, S. A., Skakle, J. M. S., Low, J. N., Wardell, J. L., Garden, S. J., Pinto, A. C., Torres, J. C. & Glidewell, C. (2001). *Acta Cryst. C* **57**, 942–945.
- Nonius (1997). *Kappa-CCD Server Software*, Windows 3.11 Version. Nonius BV, Delft, The Netherlands.
- Otwinowski, Z. & Minor, W. (1997). *Methods in Enzymology*, Vol. 276, *Macromolecular Crystallography*, Part A, edited by C. W. Carter Jr & R. M. Sweet, pp. 307–326. New York: Academic Press.
- Quesada, A., Marchal, A., Melguizo, M., Noguera, M., Sánchez, A., Low, J. N., Cannon, D., Farrell, D. M. M. & Glidewell, C. (2002). *Acta Cryst. B* **58**, 300–315.
- Sheldrick, G. M. (1997). *SHELXS97* and *SHELXL97*. University of Göttingen, Germany.
- Spek, A. L. (2003). *J. Appl. Cryst.* **36**, 7–13.
- Trask, A. V., Motherwell, W. D. S. & Jones, W. (2004). *Chem. Commun.* pp. 890–891.
- Wilson, A. J. C. (1976). *Acta Cryst. A* **32**, 994–996.